PAPER

Check for updates

Preliminary characterization of the structure and immunostimulatory and anti-aging properties of the polysaccharide fraction of *Haematococcus pluvialis*†

Xiaojuan Liu, [ID] *[ab] Miao Zhang,[ab] Han Liu,[ab] Aimei Zhou,[ab] Yong Cao[ab] and Xin Liu[ab]

In this study, a polysaccharide fraction (HPP-c3-s1) was obtained from *Haematococcus pluvialis* using DEAE-52 anion exchange and Sephacryl S400 chromatographies. The structure of HPP-c3-s1 was partially characterized and its biological activity was investigated. HPP-c3-s1 is a homogeneous polysaccharide with a molecular weight of 23 413 kDa as determined by high-performance gel permeation chromatography and polyacrylamide gel electrophoresis. Periodate oxidation and Smith degradation analysis combined with GC-MS determined that HPP-c3-s1 contains $1 \rightarrow 2$, $1 \rightarrow 3$, $1 \rightarrow 4$, and probably a few $1 \rightarrow 6$ glycosyl linkages. Fourier transform infrared spectroscopy and nuclear magnetic resonance analyses indicate HPP-c3-s1 is a pyranose containing an amino and O-acetyl group. The sugar chains in HPP-c3-s1 contain both α and β glycosidic configurations, where the β configuration is the primary form. It was observed that the HPP-c3-s1 nanostructure had linear and branched forms at a concentration of 5 μg mL^{-1} and created different sized aggregates at a higher concentration of 50 μg mL^{-1}. Furthermore, HPP-c3-s1 had significant immunostimulatory effects on splenocytes and B lymphocytes. In assays assessing anti-aging effects, HPP-c3-s1 extended the mean survival of *Caenorhabditis elegans* without adversely affecting reproduction. In addition, treatment with HPP-c3-s1 resulted in delays in age-related physiologic parameters, including body movement, rates of head swing and body bending, and accumulation of intestinal lipofuscinosis in *C. elegans*. Overall, these results suggest HPP-c3-s1 has remarkable immunomodulatory and anti-aging properties that may serve as the basis for development of functional foods and dietary supplements.

1. Introduction

In recent years, algal polysaccharides have been the focus of interest as novel bioactive materials, primarily due to their novel structures and potential biological functions.[1] Sulfated polysaccharides contain sulfated ester groups within their sugar residues, which are common components of a wide range of macroalgae (seaweeds).[2] The chemical structures vary based on the algal species and extraction procedure. Substantial studies have found these seaweed polysaccharides possess unique anticoagulant,[3] anti-inflammatory,[4] antitumor,[5] antioxidant,[6] and immunomodulating properties,[7] suggesting potential for use in pharmaceutical applications. Therefore, polysaccharides originating from red and brown macroalgae have attracted much attention as functional food additives and natural therapeutic agents in the pharmaceutical field.

Microalgae, which are distinct from macroalgae, are photosynthetic unicellular alga that utilize inorganic nutrients present in marine and fresh water, are easily cultivated, and have been investigated as foods for human consumption and attractive sources of functional food.[8] Microalgae contain an abundance of polysaccharides, some of which may possess diverse bioactivity with pharmacological significance.[9] However, fewer studies have been conducted on microalgal polysaccharides than on macroalgal polysaccharides. For example, sulfated HCP from the green microalgae *Haematococcus lacustris* has potent immunomodulating activity,[10] while sulfated EPS from the microalgae *Gyrodinium impudicum* strain KG03 has antiviral activity.[11]

Haematococcus pluvialis is a unicellular green alga found in both marine and fresh water and has garnered much attention, including in the form of studies on producing and bioengineering astaxanthin, an excellent antioxidant that can be isolated from *H. pluvialis*.[12] However, few studies have been conducted on the chemical structures and potential bioactivity

ᵃDepartment of Food Science, College of Food Science, South China Agricultural University, Guangzhou 510642, China. E-mail: liuxj@scau.edu.cn; Tel: +86-20-85286234

ᵇResearch Center of Natural Active Compound Engineering Technology of Guangdong Province, Guangzhou 510642, China

† This manuscript has been thoroughly edited by a native English speaker from an editing company.

of polysaccharides in *H. pluvialis*, although studies have determined *H. pluvialis* polysaccharides have antioxidant and thrombolytic properties.[13] Accordingly, additional searching for active polysaccharides in *H. pluvialis* aids in the development of new functional foods. For these reasons, a water-soluble polysaccharide, HPP-c3-s1, was isolated and purified from *H. pluvialis*. In the present study, the chemical structure of HPP-c3-s1 was characterized, and its immunomodulatory and anti-aging properties were assessed using several *in vitro* and *in vivo* tests.

2. Materials and methods

2.1. Materials

Dried *Haematococcus pluvialis* residue was obtained from Jingzhou Natural Astaxanthin Inc. Male BALB/c mice (6 to 8 weeks old) were purchased from the SPF Laboratory Animal Center at Southern Medical University. All animal studies were approved by South China Agricultural University Institutional Animal Care and Use Committee and performed in strict accordance of NIH guidelines for animal care. Reagents used in cell-based assays included RPMI 1640 medium, fetal bovine serum (FBS), and 100× penicillin and streptomycin purchased from Gibco (Grand Island, NY, USA), and dimethyl sulphoxide (DMSO), 3-(4,5-dimethylthiazol-2-yl)-2,5-diphenyltetrazolium bromide (MTT), concanavalin A (ConA), lipopolysaccharide (LPS), standard sugars, and dextran standard purchased from Sigma-Aldrich Co., Ltd (St. Louis, MO, USA). *Caenorhabditis elegans* wild type N2 (var. Bristol) were obtained from the Caenorhabditis Genetics Center (CGC, University of Minnesota, Minneapolis, MN, USA). The *Escherichia coli* OP50 uracil mutant was provided by the College of Resource and Environment at the South China Agricultural University. All other chemical reagents used were analytical grade.

2.2. Preparation of polysaccharide HPP-c3-s1

Crude polysaccharide (HPP) was extracted from *H. pluvialis* residues using ultrasonic-assisted extraction, anhydrous ethanol (1 : 4, v/v) precipitation, and then deproteination with Sevag reagent (*n*-butanol: chloroform = 1 : 5, v/v) as described in a previous report.[14] The HPP was purified using a DEAE-cellulose-52 chromatography column (3.0 × 35 cm) and then eluted stepwise with distilled water and a gradient of 0.1, 0.3, 0.5, and 1.0 M NaCl at a flow rate of 2 mL min⁻¹. It was further purified by Sephacryl S-400 (1.6 × 70 cm) gel permeation chromatography, where it was eluted with distilled water at a flow rate of 0.3 mL min⁻¹. One of the obtained purified polysaccharide fractions was designated HPP-c3-s1.

2.3. Determination of homogeneity and molecular weight

The homogeneity and molecular weight of HPP-c3-s1 were measured using high-performance gel permeation chromatography (HPGPC) on a LC-10A HPLC system (Shimadzu, Japan) with a RID-10A detector.[15] A gel-filtration chromatographic column system comprised of TSK-Gel G5000 PWXL and TSK-Gel G3000 PWXL columns (both 7.8 mm × 30 cm, Tosoh, Japan) connected in series were maintained at 40 °C and an injection volume of 20 μL was used. Ultra-pure water was used as the mobile phase at a flow rate of 0.6 mL min⁻¹. Dextran T-series standards of varying molecular weights (T-5000, T-12000, T-25000, T-50000, T-80000, T-150000, T-270000, T-410000, and T-670000) were prepared to estimate the molecular weight (MW) of the polysaccharide. The equation for the calibration curve of dextran was: $Y = 0.2256X^2 - 5.1357X + 33.715$ ($R^2 = 0.9887$). X: Logarithm of relative molecular mass of dextran; Y: elution volume.

The homogeneity of HPP-c3-s1 was also measured by polyacrylamide gel electrophoresis (PAGE) with 8% separating and 3.5% stacking gels. HPP-c3-s1 in boric acid-potassium chloride buffer (0.1 mL, 10 mg mL⁻¹) was mixed at a 2 : 1 ratio with sample buffer (boric acid-potassium chloride buffer, pH 9.0 containing 0.2% bromophenol blue and 40% glycerol) and centrifuged at 10 000 rpm for 5 min at 4 °C. Sample solution (10 μL) was loaded into each lane of the gel. The samples were electrophoresed initially at 40 V for 20 min and then at 110 V for 1 h. The gels were washed with a rinse solution (1 : 50 : 50 of glacial acetic acid, ethanol, and distilled water), and then oxidized with periodic acid for 40 min. The gels were then rinsed with sodium metabisulfite solution, incubated with Schiff staining solution for 30 min, and then destained with sodium metabisulfite solution three times for 5 min each. The gels were optically scanned using a Universal Hood II (Bio-rad Company, USA) gel imaging analysis system.

2.4. Periodate oxidation and smith degradation

To prepare the monosaccharide derivatives, 10.00 mg hydroxylamine hydrochloride, and 0.5 mL pyridine were added to 5.00 mg D-ribose, D-glucose, D-mannose, or D-arabinose. The tubes were filled with nitrogen gas and then sealed. The reaction was incubated at 90 °C for 30 min and then cooled. Following addition of 0.5 mL of acetic anhydride, the tubes were once again filled with nitrogen gas and then sealed. The reaction was incubated at 90 °C for another 30 min, and the saccharide acetate derivative of monosaccharide was obtained. After passing through a 0.22 μm filter, 5 μL of sample was used for GC-MS analysis.

A solution of 5 mg HPP-c3-s1 mixed with 50 mL of 15 mM NaIO₄ was kept at 4 °C in the dark. Oxidation was quenched by adding 1.5 mL ethylene glycol after 24 h. The solution was concentrated, reduced, neutralized, dialyzed, and lyophilized to produce a degraded product. This degraded product (2 mg dissolved in 2 mL of water) was further hydrolyzed with 4 M trifluoroacetic acid at 110 °C for 3 h in a screw cap tube filled with nitrogen gas. Hydroxylamine hydrochloride (10 mg) and 0.5 mL of pyridine were added to the hydrolyzed samples and the samples incubated for 30 min at 90 °C. Next, 0.5 mL of acetic anhydride was added and the samples were allowed to stand again for 30 min at 90 °C.[16] The resulting alditol acetate product was analyzed by GC-MS. For GC-MS, a DB-5 column (0.2 mm × 30 m × 0.25 μm) and high purity helium as a carrier gas were used. The flow rate was 1.2 mL min⁻¹, the chromatographic inlet temperature 280 °C, and the column temperature program was set at an initial temperature of 120 °C for 5 min followed by

a temperature rise at 120 °C at a rate of 20 °C min^{-1} for 5 min, and then a temperature increase to 280 °C at a rate of 10 °C min^{-1} for 5 min. For mass spectrometry, an EI ion source was used, the electron energy was 70 eV, and the transmission line temperature was 280 °C.[17]

2.5. Fourier transform infrared spectroscopy (FTIR)

FTIR spectroscopy was used to analyze the structure of purified HPP-c3-s1. To this end, 1 mg of solid sample was mixed with dry potassium bromide (100 mg) and then analyzed on a Nexus FTIR (Nicolet Nexus, Thermo Nicolet Company, USA) with a DTGS KBr detector. The absorptive spectra were recorded in the frequency range of 4000–400 cm^{-1}.[18]

2.6. Nuclear magnetic resonance (NMR)

The ^{1}H NMR spectra of HPP-c3-s1 were recorded using an Avance© NMR spectrometer (Bruker, Germany) at 600 MHz in D$_2$O. Freeze-dried sample (10 mg) was exchanged three times with D$_2$O and spectra were measured in the range of 0–6 ppm.[19]

2.7. Atomic force microscope (AFM)

The nanostructure and self-assembly capability of HPP-c3-s1 were determined by AFM. HPP-c3-s1 suspensions were prepared with concentrations of 5 and 50 μg mL^{-1}. Exactly 5 μL of each sample was dropped onto freshly cleaved mica and air dried overnight. AFM imaging was performed on a MultiMode 8 (Bruker, Germany) instrument at room temperature (approximately 22–25 °C) and a relative humidity of 50–60% on a mica sheet. The tape on the tip was Silicon Tip on Nitride Lever and the cantilever was RTEST (T: 650 nm, f_0: 70 kHz, k: 0.4 N m^{-1}).[20]

2.8. Spleen lymphocyte proliferation assay

Splenocytes were harvested from mice and then suspended in RPMI-1640 medium. Splenocytes were transferred to a 96-well culture plate at 1.0×10^6 cells per mL in 200 μL complete medium. Each well was treated with 25 μL of 3.9, 7.8, 15.6, 31.2, 62.5, 125, or 250 μg mL^{-1} polysaccharide. The plates were incubated at 37 °C in a humidified 5% CO$_2$ atmosphere. Cells were treated with 25 μL of 10 μg mL^{-1} ConA or 10 μg mL^{-1} LPS as positive controls. Meanwhile, the blank control was treated with 25 μL of the medium. After 44 h, 20 μL of 5 mg mL^{-1} MTT was added to each well and the plates were incubated for another 4 h. The plates were centrifuged at 3000 rpm for 10 min, the supernatant was discarded, and then 150 μL of DMSO was added to dissolve formazan crystals. The absorbance of the splenocytes in each well was measured at 570 nm using a microplate reader (ThermoScientific Instruments, USA).[21]

2.9. Preparation of treatment plates

HPP-c3-s1 was dissolved in sterile water to final concentrations of 50, 200, and 400 μg mL^{-1} according to our pre experiment. Each concentration of HPP-c3-s1 was freshly spotted onto a 60 mM Petri dish containing 10 mL of nematode growth medium (NGM). All HPP-c3-s1 plates were seeded with $E.\ coli$ OP50 one day before use. The plates were stored at 4 °C.

2.10. Lifespan assay

$C.\ elegans$ were cultured and maintained at 20 °C on NGM plates seeded with $E.\ coli$ OP50 as previously described.[22] All treatments started at the L4 stage after synchronizing with sodium hypochlorite, which kills adult worms but not their eggs. For each treatment, 90 nematodes were transferred to NGM plates previously treated with corresponding test concentrations of HPP-c3-s1 or $E.\ coli$ OP50 alone as a control. The first day of adulthood was designated day 0 and nematodes were transferred to fresh treatment plates every 2 days to avoid contamination. The survival of the nematodes was noted daily until all the worms had died. Any worms that fled to the wall or cover of the Petri dish and died or drilled into the agar were excluded from the analysis.[22] Three independent trials were performed per treatment. Data are shown as mean lifespan per trial.

2.11. Measurement of age-related changes in physiological processes

Mobility force assay were performed as previously described.[23] For the egg-laying assay, L4 larvae ($n = 10$ for each treatment) were placed on individual plates with a treatment or control and then transferred to fresh plates every 24 h until reproduction ceased. The progeny of each nematode were enumerated at the L2 or L3 stage.[24] The rate of head swing and body bending were determined by counting head swings and sinusoidal motions, respectively. The nematodes were grown on NGM plates containing a treatment or control. Ten nematodes were randomly selected on days 5, 10, and 15, and the rates of head swings and body bending were recorded at for regular intervals of 30 s and 1 min, respectively. Each experiment was performed independently in triplicate.

2.12. Statistical analysis

Experimental results are expressed as mean ± SD. Statistically significant differences were determined by one-way ANOVA using SPSS 17.0 (IBM Co., NY, USA). Statistical significance was considered $p < 0.05$.

3. Results and discussion

3.1. Homogeneity and molecular weight of HPP-c3-s1

As shown in Fig. 1A, HPGPC analysis revealed only one single and symmetrical peak for the purified polysaccharide, HPP-c3-s1, indicating it was a homogeneous fraction. This peak had a retention time of 12.633 min. According to the calibration curve, $\log M_w = -0.2073R_t + 9.7969$, where $R^2 = 0.995$, M_w is standard molecular weight, and R_t represents retention time, the average molecular weight of HPP-c3-s1 was calculated to be about 23 413 kDa. Based on PAGE, HPP-c3-s1 had a single PAS-positive band (Fig. 1B), which suggests HPP-c3-s1 is a homogeneous polysaccharide. The PAGE results supported the HPGPC analysis.
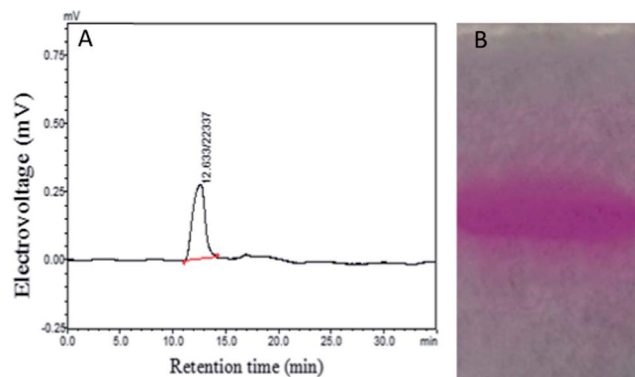
Fig. 1 The homogeneity and molecular weight of HPP-c3-s1 were investigated using HPGPC (A) and PAGE (B). The spectrum of HPP-c3-s1 was determined through a LC-10A HPLC system equipped with a RID-10A detector. Ultra-pure water was used as the mobile phase at a flow rate of 0.6 mL min⁻¹. The column temperature was 35 °C and the injection volume was 20 μL. Electropherogram of HPP-c3-s1, stained according to the periodic acid-Schiffs reagent (PAS) method. The separating and stacking gel solutions were 8% and 3.5%, respectively. Electrophoresis of samples was initially at 40 V for 20 min and then at 110 V for 1 h. The gels were rinsed, oxidized, rinsed, stained, destained, and scanned according to Material and methods 2.3.

3.2. Periodate oxidation and smith degradation analysis

Upon periodate oxidation, HPP-c3-s1 produced 0.0028 mmol formic acid, indicating the likely presence of $1 \rightarrow 6$ glycosyl linkage(s). Based on the sodium periodate calibration curve, 0.0287 mmol of sodium periodate was consumed during oxidation. The consumption of sodium periodate being more than twice the amount of formic acid produced indicates there may be numerous glycosyl linkages, such as $1 \rightarrow 2$ and $1 \rightarrow 4$, because these two linkages consume sodium periodate, but produce no formic acid.[25]

After Smith degradation of the periodate-oxidized product, the degradation products were examined by GC-MS (Fig. 2). Ribose, glucose, and mannose were present, indicating the presence of corresponding linkages that could not be oxidized, namely $1 \rightarrow 3$ linkages. In addition, glycerol was found in the degradation products, suggesting the presence of glycosidic linkages, such as $1 \rightarrow 2$ or $1 \rightarrow 6$. Erythritol was also present, revealing HPP-c3-s1 may contain a $1 \rightarrow 4$ linkage. Therefore, the results from periodate oxidation-Smith degradation suggest that HPP-c3-s1 contains $1 \rightarrow 2$, $1 \rightarrow 3$, $1 \rightarrow 4$, and small number of $1 \rightarrow 6$ linkages.
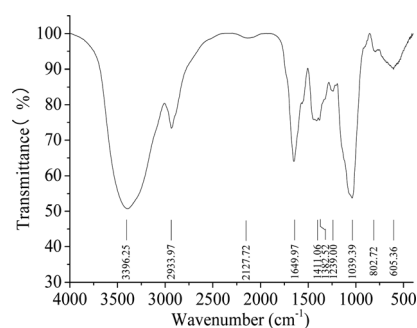
3.3. FTIR spectroscopy

The FTIR spectrum of HPP-c3-s1 contained bands characteristics of polysaccharides with absorbance modes from 400 to 4000 cm⁻¹ (Fig. 3). The intense and broad band at 3396.25 cm⁻¹ was from the stretching vibration of an O–H, suggesting the presence of intra- and intermolecular hydrogen bonds. The absorption peaks at 2933.97 and 1200 to 1400 cm⁻¹ correspond to the stretching and angular vibration of a C–H bond, indicating HPP-c3-s1 is a carbohydrate.[26] The moderate strength absorption peak around 1649.97 cm⁻¹ was from C=O stretching vibration, suggesting that HPP-c3-s1
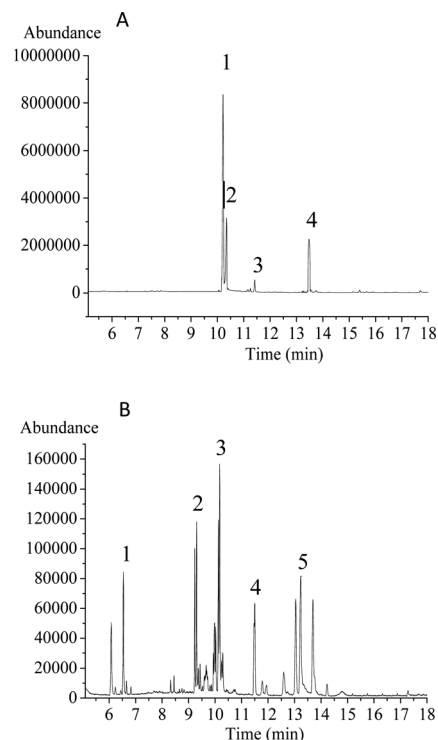
Fig. 2 GC-MS profiles of derivatives of monosaccharide standards (A) and Smith degradation products of HPP-c3-s1 (B). The monosaccharide standards and samples were treated according to Material and methods 2.4. The GC-MS conditions were as follows: carrier gas, high purity helium; flow rate, 1.2 mL min⁻¹; EI ion source; electron energy, 70 eV; transmission line temperature, 280 °C. (A) Four monosaccharide standards. (1) Ribose (Rib); (2) arabinose (Ara); (3) mannose (Man); (4) glucose (Glc); (B) HPP-c3-s1. (1) Glycerol; (2) erythritol; (3) ribose (Rib); (4) mannose (Man); (5) glucose (Glc).

may contain acetyl or uronic acid groups. The absorption peak at 1411.06 cm⁻¹ likely relates to C–H bending vibration, while the band at 1239.00 cm⁻¹ can be assigned to the stretching of an S=O bond. The strong absorption peak at 1039.39 cm⁻¹ is from C–O stretching in a primary alcohol OH, which is the characteristic absorption peak of the pyranose carbohydrate ring.[27] These results indicate that HPP-c3-s1 is a sulphated pyranose.

Fig. 3 Fourier transform infrared spectroscopy analysis of the HPP-c3-s1 fraction. Sample, 1 mg, mixed with potassium bromide (100 mg) was analyzed on a Nexus FTIR with a DTGS KBr detector. The absorptive spectra were recorded in the frequency range of 4000–400 cm⁻¹.

3.4. Analysis of ^{1}H NMR spectroscopy

To verify the characteristic chemical shifts and corresponding functional groups of HPP-c3-s1, ^{1}H NMR spectroscopy was used (Fig. 4). There were anomeric hydrogen signals between δ 3.0 and 5.0 ppm. The chemical shifts of C1 protons at less than and more than 5.0 ppm can be attributed to then β- and α-anomeric configurations, respectively, confirming both α and β configurations may be present in HPP-c3-s1.[28] TPC3-1 molecule from green tea (*Camellia sinensis* L.) also has the anomeric carbon signs of both α and β configurations.[29] The residual hydrogen of D$_2$O was observed at 4.70 ppm and the signal at 4.01 ppm was related to the hydrogen next to the functional –OH group. A group of overlapping signals between δ 3.3 and 4.0 ppm correspond to C2–C6 protons, which was difficult to analyze. Spectra at around δ 1.93 and 2.12 ppm suggest the presence of acetyl groups. The signals between δ 0.99 and 3.66 ppm indicate an amino group.[30] No characteristic chemical shift was observed near δ 5.4 ppm, indicating HPP-c3-s1 is a pyranose. Due to the absence of ^{13}C NMR data, linkage data on the sugar chains is unclear.

3.5. Atomic force microscopy of HPP-c3-s1

Fig. 5 presents the nanostructural properties of HPP-c3-s1, where two different concentrations, 5 and 50 μg mL^{-1}, of the material were used for AFM. At a concentration of 50 μg mL^{-1}, HPP-c3-s1 formed different sized small aggregates with an average diameter of 80–150 nm (Fig. 5A). Spontaneous aggregates with spherical and looped structures, as well as linear and branched forms, formed at the 5 μg mL^{-1} concentration (Fig. 5B). Fig. 5C (5 μg mL^{-1}) clearly presents that HPP-c3-s1 contained both linear and branched structures, where the width of the linear molecules ranged from 23 to 36 nm and the height from about 0.6 to 1.5 nm. According to periodate oxidation, Smith degradation analysis, and FTIR spectroscopy, HPP-c3-s1 formed through branched chains. This corresponded with the small aggregates and linear and branched structures observed on AFM. In recent years, some reports described the use of AFM to determine the molecular structure of polysaccharides. CP2-c2-s2 from *Cordyceps militaris* showed different aggregates and networks from 5 μg mL^{-1} to 250 μg mL^{-1}. At low concentrations (5 μg mL^{-1}), the

Fig. 4 ^{1}H NMR spectra of HPP-c3-s1. The spectra were recorded using an Avance II NMR spectrometer at 600 MHz in D$_2$O. Freeze-dried sample, 10 mg, was exchanged three times with D$_2$O and spectra were measured in the range of 0–6 ppm.
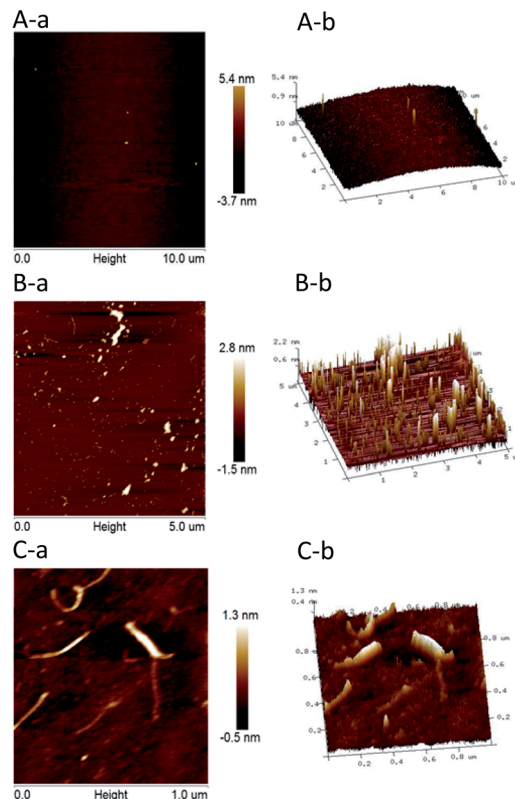
Fig. 5 AFM images of HPP-c3-s1 at concentrations of (A) 50 μg mL^{-1}, (B) 5 μg mL^{-1}, and (C) 5 μg mL^{-1}. (a) Height mode image; (b) 3D visualization. Exactly 5 μL of each sample was dropped onto freshly cleaved mica and air-dried overnight. AFM imaging was recorded on MultiMode 8 instrument at room temperature of about 22–25 °C and a relative humidity of 50–60% on mica sheet. The tape of the tip was Silicon Tip on Nitride Lever and the cantilever was RTEST (T: 650 nm, f0: 70 kHz, k: 0.4 N m^{-1}).

CP2-c2-s2 molecules formed small dispersed aggregates with different sizes. At 50 μg mL^{-1} clearly formed rod-like helical network structures.[31] AMBG from *Mesona blumes* gum showed spherical lumps at 1 μg mL^{-1} but an irregular worm-like shape at 10 μg mL^{-1}.[32]

Determining the polysaccharide chemical structure and analysis of the carbohydrate chain were very difficult. At present, most studies on polysaccharide structure concentrate on the primary structure. Because polysaccharides have a large relative molecular weight, the sugar residues are often connected with methyl, acetyl, sulfate, and phosphate groups, rendering the primary structure of polysaccharides complex and difficult to analyse. Nevertheless, structural analysis plays an important role in the study of polysaccharides. It is also the basis of the relationship between the molecular structure and biological functions of polysaccharides. At present, there are many methods to analyze polysaccharide structure and typical methods, including chemical analysis, such as acid hydrolysis method, periodate oxidation, and Smith degradation, and instrumental analysis, such as infrared spectroscopy, NMR, and GC/MS.[33] In this study, chemical analysis in the forms of periodate oxidation and Smith degradation, as well as instrumental
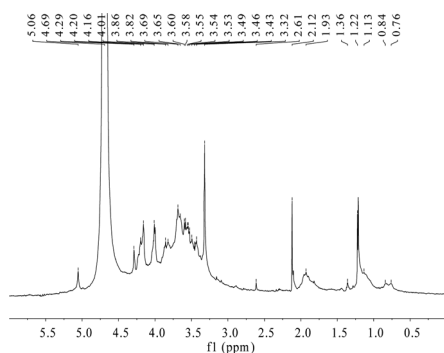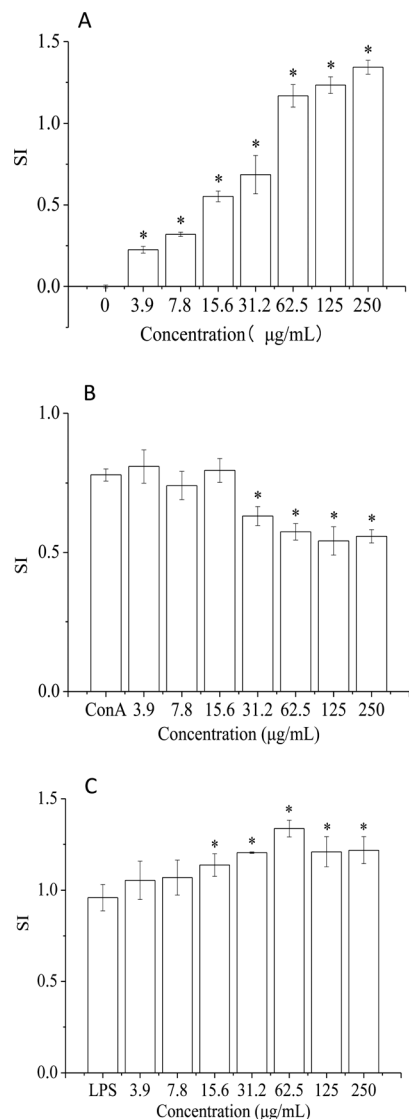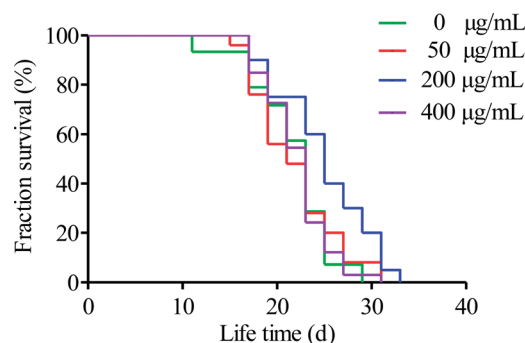
Fig. 6 Effects of HPP-c3-s1 on mouse splenocyte lymphocyte simulation: (A) polysaccharide stimulation alone, (B) ConA-induced T lymphocytes, and (C) LPS-induced B lymphocytes. After 44 h, the cell viability was measured by MTT assay. Each value was presented as mean ± SD, (n = 6). *p < 0.05 compared to positive control.

### 3.6. Effect of HPP-c3-s1 on spleen lymphocyte proliferation

The immune system has a crucial role in health and consists of tissues, cells, and molecules that protect organisms from infections.[34] In recent years, alga polysaccharides have been shown to modulate the human immune system and protect human health.[35] In this study, the effect of HPP-c3-s1 on splenic lymphocytes was investigated to characterize its mechanism of the immunoregulatory activity. As shown in Fig. 6, treatment with HPP-c3-s1 significantly increased splenocyte and B lymphocyte proliferation. However, HPP-c3-s1 had no effect on the proliferative activity of ConA-induced T lymphocytes at doses of 3.9 to 250 μg mL^{-1} compared to the ConA alone group. Even at the doses of 31.2 to 250 μg mL^{-1}, HPP-c3-s1 had significantly decrease the proliferative activity of ConA-induced T lymphocytes. The possible reason was that the high concentration of polysaccharide and ConA caused overstimulation of cells under the synergistic effect, thus inhibiting the proliferation of cells. The specific reasons are still to be studied further. At doses of 15.6 to 250 μg mL^{-1}, HPP-c3-s1 significantly promoted splenocyte and LPS-stimulated splenocyte proliferation, indicating that HPP-c3-s1 is directly mitogenic for B lymphocytes. The SI (Stimulus Index) of 62.5 μg mL^{-1} HPP-c3-s1 in LPS-induced B lymphocytes was 1.34 (Fig. 6C). However, at doses of HPP-c3-s1 higher than 62.5 μg mL^{-1}, B lymphocyte proliferation gradually decreased. These results indicate that HPP-c3-s1 has remarkable immunostimulatory activity, where HPP-c3-s1 promotion of lymphocyte proliferation is mainly through LPS-induced B lymphocyte proliferation.

The immune system prevents diseases through biological processes. Diseases of the immune system can lead to autoimmunity, inflammation, and even cancer. The spleen is an important peripheral immune organ and is where immune cells perform a number of their immune-related functions. Splenic cells consist of several types of immune cells, including T and B lymphocytes, which can directly respond to the immune regulation of the organism.[36] T and B lymphocytes are two important types of immunologically active cells. The former is mainly responsible for cellular immunity, while the latter are the only cells that produce antibodies and are the primary humoral immune cells.[37] ConA and LPS are mitogenic agents for T cells

analysis through HPGPC, IR, NMR, GC/MS, and AFM, were used to determine the primary structure of HPP-c3-s1. The primary structure of polysaccharide HPP-c3-s1 is composed of four monosaccharides, including D-ribose, D-arabinose, D-mannose, and D-glucose with $1 \rightarrow 2$, $1 \rightarrow 3$, $1 \rightarrow 4$, and trace amounts of $1 \rightarrow 6$ glycosidic linkages. HPP-c3-s1 is a pyranose containing an amino and an O-acetyl group. The sugar chains contain two glycosidic configurations, α and β, and are primarily in the β configuration. It was observed the HPP-c3-s1 nanostructure contains linear and branched forms at a concentration of 5 μg mL^{-1}, and different sized aggregates at a higher concentration of 50 μg mL^{-1}. This important information aids in revealing the primary and advanced structures of the polysaccharide isolated from *H. pluvialis*.

Fig. 7 Effects of HPP-c3-s1 at concentrations of 50, 200, and 400 μg mL^{-1} on lifespan extension of *C. elegans*. Day 0 refers to the first day that *C. elegans* (L4 stage) were transferred to NGM plates. Worms were scored daily for survival. Three independent trials were performed.
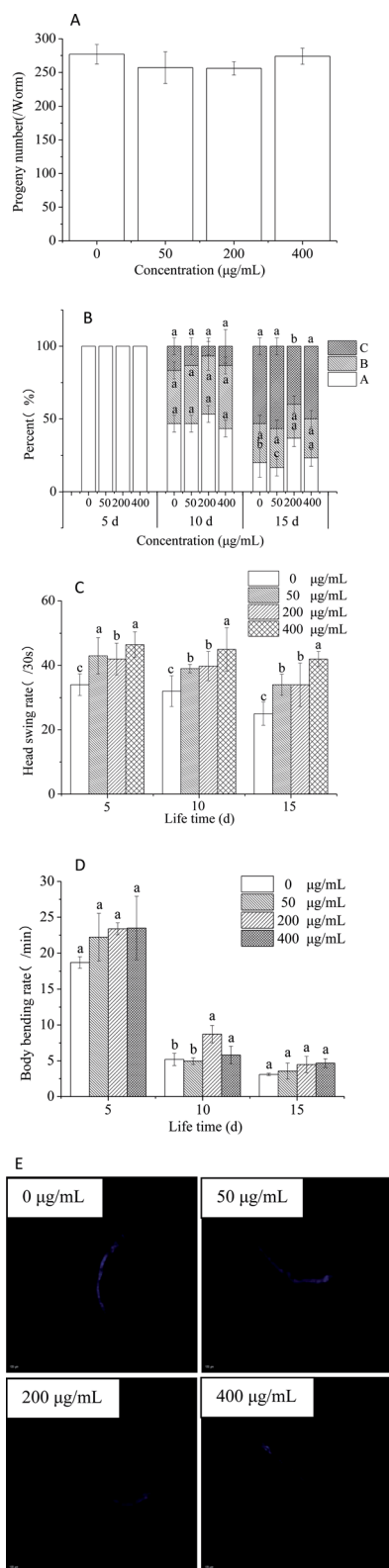
Fig. 8 Effects of different concentrations of HPP-c3-s1 on age-related changes in physiologic parameters of *C. elegans*. The fecundity (A), body movement (B), head swing rate (C), and body bending rates (D) were counted under a dissecting microscope. (E) The intestinal lipofuscin fluorescence of day 8 worms was photographed using a fluorescence microscope. The lipofuscin level was quantified using ImageJ software by determining the average pixel intensity in each worm. The experiment was repeated three times and images were captured using a 20× objective. Data are expressed as the mean ± SD, ($n = 3$). The data were statistically analyzed using one way-ANOVA (SPSS 17.0). Differences between the data were considered significant at $p < 0.05$.

and B cells, respectively. It is generally accepted that drugs capable of enhancing ConA- or LPS-promotion of spleen cell proliferation act through promotion of proliferation of T or B cells. Studies have shown that a polysaccharide from *Spirulina* not only stimulated the proliferation of lymphocytes and induced the secretion of IL-2 in mouse spleen cells, but also promoted transformation of these cells *in vitro* following induction by ConA in a dose-dependent manner.[38] Treatment of mice immunocompromised with cyclophosphamide treatment with *Spirulina* polysaccharide displayed a significant promotion in proliferation of spleen cells and thymocytes. *Spirulina* polysaccharide significantly enhanced the transformation of mouse spleen lymphocytes induced by ConA, thus enhancing the immune activity of immune cells.[39] In addition, a high-molecular-weight polysaccharide extract from the cyanobacterium *Arthrospira platensis* enhanced human adaptive immune responses.[40] A new low molecular weight sulfated polysaccharide GLP-2 isolated from *Gracilaria lemaneiformis* significantly improved the proliferation and pinocytosis of RAW264.7 cells and promoted the production of reactive oxygen species, nitric oxide, interleukin-6, and tumor necrosis factor-alpha by activating expression of inducible nitric oxide synthesis, interleukin-6, and tumor necrosis factor-alpha.[41] In this paper, the proliferation of T and B lymphocytes was studied in terms of enhancement of immune activity by HPP-c3-s1. It was found that HPP-c3-s1 not only independently stimulated spleen cell proliferation, but certain concentrations also significantly promoted mouse spleen B lymphocyte LPS-induced proliferation in a dose-dependent manner. These results show that HPP-c3-s1 binds to the B lymphocyte receptor and plays a role similar to that of LPS mitogen, thus stimulating B lymphocyte proliferation. However, no such activity was observed for T lymphocytes. In addition, the effect of high concentrations of polysaccharide on cell proliferation under synergistic action inhibited proliferation, although the mechanism behind this remains to be delineated.

3.7. Anti-aging activity

C. elegans can quickly perceive external environmental factors, such as light, heat, heavy metals, and poisons. It is an excellent model organism that is very sensitive to the environment. At present, it is widely used in the field of medicine and basic biological research.[42] Up to now, there are few studies on the anti-aging activity of microalgae polysaccharides using *C. elegans* model. Polysaccharides from Chinese traditional herbal medicines, including *Cordyceps militaris*,[31] *Bletilla striata*,[43] and *Panax notoginseng*,[44] have been shown to extend the lifespan of *C. elegans*. When evaluating nematode aging, lifespan is the main index used.[45]

To evaluate the effect of HPP-c3-s1 on the lifespan of *C. elegans*, N2 wild type nematodes were treated with concentrations

of 50, 200, and 400 μg mL^{-1}. Treatment with 200 μg mL^{-1} HPP-c3-s1 extended the mean survival of the worms, while 50 and 400 μg mL^{-1} had no obvious effect compared to the control group (Fig. 7). It was observed that 200 μg mL^{-1} HPP-c3-s1 significantly increased the average lifespan of the nematodes by 14.92% ($p < 0.05$) and the maximum life increased by about 3.33 d. While 50 and 400 μg mL^{-1} HPP-c3-s1 had no significant effect on the mean lifespan of worms ($p > 0.05$), they did increase the maximum lifespan of the worms.

Several physiologic parameters, including fecundity, body movement, rates of head swings and body bending, and intestinal lipofuscinosis, were also observed to evaluate the anti-aging activity.[46] None of the treatment groups displayed significant variation in progeny production. Thus, HPP-c3-s1 had no impact on reproduction in *C. elegans* (Fig. 8A). Motility classes were determined by scoring the locomotion phenotype of worms by gently prodding them with a platinum wire. 'A' worms move spontaneously away from the touch; 'B' worms did respond to touch, but with somewhat uncoordinated and move slowly; 'C' worms were unable to move, but they were clearly alive. On day 5, all the groups of worms could move spontaneously without touching a stimulus, *i.e.* displayed movement. On day 10, the proportion of nematodes in state A of each group began to decrease, while those in state B significantly increased (Fig. 8B). In addition, the number of nematodes in state A in the 200 μg mL^{-1} HPP-c3-s1 was higher than in the other three groups and exhibited significant difference compared with the control group on day 15 ($p < 0.05$). These results demonstrate HPP-c3-s1 slows down deterioration of motility in the worms. We observed a decline in the rate of head swing on days 5, 10, and 15 for both the treated (HPP-c3-s1) and untreated N2 worms, however the rate in the treated group remained significantly higher than the control group ($p < 0.05$). Moreover, the rate of head swing in the worms treated with 400 μg mL^{-1} HPP-c3-s1 was much higher than in the other three groups, suggesting that HPP-c3-s1 plays a significant role in delaying the rate of head swing in nematodes (Fig. 8C). The mean body bending rate decreased within 15 days (Fig. 8D). Compared to the control group, the mean body bending rate slightly increased in the HPP-c3-s1-treated group on days 5 and 15. However, treatment with 200 μg mL^{-1} HPP-c3-s1 significantly increased the rate of body bending ($p < 0.05$). Intracellular lipofuscin level is a prominent marker for aging and age-related cellular damage.[47] To measure intestinal lipofuscin accumulation, ImageJ software was used to calculate levels in worms on day 8 (Fig. 8E). It was found 200 μg mL^{-1} HPP-c3-s1 significantly reduced lipofuscin fluorescence compared to the control group ($p < 0.05$). Therefore, HPP-c3-s1 partly decreased the accumulation of intestinal lipofuscin and, thus, extended the lifespan of nematode.

4. Conclusions

In summary, the aqueous polysaccharide HPP-c3-s1 was isolated from the microalgae *H. pluvialis* and determined to have a molecular weight of 23 413 kDa in this study. HPP-c3-s1 was characterized as a pyranose containing $1 \rightarrow 2$, $1 \rightarrow 4$, $1 \rightarrow 3$,

and probably a few $1 \rightarrow 6$ glycosyl linkages, an amino group, and an O-acetyl group The sugar chain contains both α and β glycosidic configurations, but primarily consists of the β configuration. Furthermore, when HPP-c3-s1 is at a concentration of 5 μg mL^{-1}, both linear and branched structures exist, where the width of the linear molecules ranges from 23 to 36 nm and the height from about 0.6 nm to 1.5 nm. By contrast, when HPP-c3-s1 was at a concentration of 50 μg mL^{-1}, small aggregates of different sizes with an average diameter of 80–150 nm formed. In addition, HPP-c3-s1 exhibited immunostimulatory effects on splenocyte lymphocytes, particularly B lymphocytes. In anti-aging assays using *C. elegans,* HPP-c3-s1 extended the mean survival without adversely impact reproduction. Furthermore, HPP-c3-s1 could alleviate the decline in physiological function caused by senility in *C. elegans*, such as body movement, rates of head swings and body bending, and accumulation of intestinal lipofuscinosis. Therefore, HPP-c3-s1 displayed remarkable immunomodulatory and anti-aging activity, indicating that HPP-c3-s1 has the potential to be used as a novel functional food.

Conflicts of interest

There are no conflicts to declare.

Acknowledgements

References

1 (*a*) L. Song, X. L. Chen, X. D. Liu, F. B. Zhang, L. F. Hu, Y. Yue, K. C. Li and P. C. Li, Characterization and comparison of the structural features, immune-modulatory and anti-avian influenza virus activities conferred by three algal sulfated polysaccharides, *Mar. Drugs*, 2016, **14**(1), 4; (*b*) A. Ekelhof and M. Melkonian, Microalgal cultivation in porous substrate bioreactor for extracellular polysaccharide production, *J. Appl. Phys.*, 2017, **29**(3), 1115–1122; (*c*) E. Hussain, L. J. Wang, B. Jiang, S. Riaz, G. Y. Butt and D. Y. Shi, A review of the components of brown seaweeds as potential candidates in cancer therapy, *RSC Adv.*, 2016, **6**(15), 12592–12610.

2 (*a*) D. H. Ngo and S. K. Kim, Sulfated polysaccharides as bioactive agents from marine algae, *Int. J. Biol. Macromol.*, 2013, **62**(11), 70; (*b*) T. H. Silva, A. Alves, E. G. Popa, L. L. Reys, M. E. Gomes, R. A. Sousa, S. S. Silva, J. F. Mano and R. L. Reis, Marine algae sulfated polysaccharides for tissue engineering and drug delivery approaches, *Biomatter*, 2012, **2**(4), 278; (*c*) A. C. M. Leodido, L. E. C. Costa, T. S. L. Araujo, D. S. Costa, N. A. Sousa, L. K. M. Souza, F. B. M. Sousa, M. D. S. Filho, D. F. P. Vasconcelos and F. R. P. Silva, Anti-diarrhoeal

therapeutic potential and safety assessment of sulphated polysaccharide fraction from *Gracilaria* intermedia seaweed in mice, *Int. J. Biol. Macromol.*, 2017, **97**, 34–45.

3 C. Faggio, M. Pagano, A. Dottore, G. Genovese and M. Morabito, Evaluation of anticoagulant activity of two algal polysaccharides, *Nat. Prod. Res.*, 2016, **30**(17), 1934–1937.

4 I. P. S. Fernando, J. W. Nah and Y. J. Jeon, Potential anti-inflammatory natural products from marine algae, *Environ. Toxicol. Pharmacol.*, 2016, **48**, 22–30.

5 E. Hussain, L. J. Wang, B. Jiang, S. Riaz, G. Y. Butt and D. Y. Shi, A review of the components of brown seaweeds as potential candidates in cancer therapy, *RSC Adv.*, 2016, **6**(15), 12592–12610.

6 M. Takei, T. Kuda, M. Eda, A. Shikano, H. Takahashi and B. Kimura, Antioxidant and fermentation properties of aqueous solutions of dried algal products from the Boso Peninsula, Japan, *Food Biosci.*, 2017, **19**, 85–91.

7 H. W. Chen, T. S. Yang, M. J. Chen, Y. C. Chang, E. I. C. Wang, C. L. Ho, Y. J. Lai, C. C. Yu, J. C. Chou and L. K. P. Chao, Purification and immunomodulating activity of C-phycocyanin from *Spirulina platensis* cultured using power plant flue gas, *Process Biochem.*, 2014, **49**(8), 1337–1344.

8 (*a*) J. Matos, C. Cardoso, N. M. Bandarra and C. Afonso, Microalgae as healthy ingredients for functional food: a review, *Food Funct.*, 2017, **8**(8), 2672–2685; (*b*) C. E. C. C. Ejike, S. A. Collins, N. Balasuriya, A. K. Swanson, B. Mason and C. C. Udenigwe, Prospects of microalgae proteins in producing peptide-based functional foods for promoting cardiovascular health, *Trends Food Sci. Technol.*, 2017, **59**, 30–36.

9 (*a*) J. Qi and S. M. Kim, Characterization and immunomodulatory activities of polysaccharides extracted from green alga *Chlorella ellipsoidea*, *Int. J. Biol. Macromol.*, 2017, **95**, 106–114; (*b*) Y. Sun, H. Wang, G. Guo, Y. Pu and B. Yan, The isolation and antioxidant activity of polysaccharides from the marine microalgae *Isochrysis galbana*, *Carbohydr. Polym.*, 2014, **113**, 22–31; (*c*) L. Sun, L. Wang and Y. Zhou, Immunomodulation and antitumor activities of different-molecular-weight polysaccharides from *Porphyridium cruentum*, *Carbohydr. Polym.*, 2012, **87**(2), 1206–1210; (*d*) S. Santoyo, M. Plaza, L. Jaime, E. Ibañez, G. Reglero and F. G. Señorans, Pressurized liquid extraction as an alternative process to obtain antiviral agents from the edible microalga *Chlorella vulgaris*, *J. Agric. Food Chem.*, 2010, **58**(15), 8522.

10 J. K. Park, Z. H. Kim and C. G. Lee, Characterization and immunostimulating activity of a water-soluble polysaccharide isolated from *Haematococcus lacustris*, *Biotechnol. Bioprocess Eng.*, 2011, **16**(6), 1090–1098.

11 C. K. Lee, H. S. Kim, R. N. Ju, J. R. Nam, M. J. Lee, J. H. Yim, H. K. Lee and E. De Clercq, Anti-picornavirus activity and other antiviral activity of sulfated exopolysaccharide from the marine microalga *Gyrodinium impudicum* strain KG03, *Antiviral Research*, 2009, **82**(2), A40.

12 G. Panis and J. R. Carreon, Commercial astaxanthin production derived by green alga *Haematococcus pluvialis*: A microalgae process model and a techno-economic assessment all through production line, *Algal Res.*, 2016, **18**, 175–190.

13 (*a*) Y. Liu, S. H. Wang and Y. Liu, Physicochemical properties and antioxidant activity of polysaccharide from *Haematococcus pluvialis* extracted by three different methods, *Food Sci. (Beijing)*, 2015, **36**(6), 161–168; (*b*) Y. M. Feng, Extraction, isolation, structural characterization and anticoagulation of polysaccharides from four kinds of green seaweeds, *J. Ocean Univ. China*, 2012.

14 M. Zhang, X. J. Liu and X. Liu, Optimization of process in extracting polysaccharide assisted by ultrasonic wave from *Haematococcus pluvialis* residues, *Food Sci. Technol. Int.*, 2016, **37**(20), 254–258.

15 X. Liu, Y. Huang, Y. Chen and Y. Cao, Partial structural characterization, as well as immunomodulatory and anti-aging activities of CP2-c2-s2 polysaccharide from *Cordyceps militaris*, *RSC Adv.*, 2016, **6**, 104094–104103.

16 D. Luo, X. Yuan, Y. Zeng, K. Nie, Z. Li and Z. Wang, Structure elucidation of a major fucopyranose-rich heteropolysaccharide (STP-II) from *Sargassum thunbergii*, *Carbohydr. Polym.*, 2016, **143**, 1–8.

17 Y. Y. Ren, Z. Y. Zhu, H. Q. Sun and L. J. Chen, Structural characterization and inhibition on alpha-glucosidase activity of acidic polysaccharide from *Annona squamosal*, *Carbohydr. Polym.*, 2017, **174**, 1–12.

18 Y. Han, J. Wu, T. Liu, Y. Hu, Q. Zheng, B. Wang, H. Lin and X. Li, Separation, characterization and anticancer activities of a sulfated polysaccharide from *Undaria pinnatifida*, *Int. J. Biol. Macromol.*, 2015, **83**(3), 42–49.

19 A. Mishra, K. Kavita and B. Jha, Characterization of extracellular polymeric substances produced by microalgae *Dunaliella salina*, *Carbohydr. Polym.*, 2011, **83**(2), 852–857.

20 D. Tang, P. Attar, A. Q. Li and E. H. Dowell, Complex dynamics of a pyranose ring structure molecule attached to an atomic force microscope, *Nonlinear Dyn.*, 2006, **45**(3–4), 283–303.

21 X. Chen, W. Nie, S. Fan, J. Zhang, Y. Wang, J. Lu and L. Jin, A polysaccharide from *Sargassum fusiforme* protects against immunosuppression in cyclophosphamide-treated mice, *Carbohydr. Polym.*, 2012, **90**(2), 1114–1119.

22 A. Pant, S. K. Saikia, V. Shukla, J. Asthana, B. A. Akhoon and R. Pandey, Beta-caryophyllene modulates expression of stress response genes and mediates longevity in *Caenorhabditis elegans*, *Nonlinear Dyn.*, 2014, **57**(9), 81–95.

23 E. M. Vayndorf, S. S. Lee and R. H. Liu, Whole apple extracts increase lifespan, healthspan and resistance to stress in *Caenorhabditis elegans*, *J. Funct. Foods*, 2013, **5**(3), 1235–1243.

24 X. Liu, Q. Luo, Y. Cao, T. Goulette, X. Liu and H. Xiao, Mechanism of different stereoisomeric astaxanthin in resistance to oxidative stress in *Caenorhabditis elegans*, *J. Food Sci.*, 2016, **81**(9), H2280–H2287.

25 T. Feng, Z. B. Gu and Z. Y. Jin, Structural studies of an acidic polysaccharide of Mesona blumes gum, *J. Sci. Food Agric.*, 2008, **88**(1), 24–34.

26 L. Wang, H. M. Liu and G. Y. Qin, Structure characterization and antioxidant activity of polysaccharides from Chinese quince seed meal, *Food Chem.*, 2017, **234**, 314–322.

27 W. Liu, Y. M. Liu, R. Zhu, P. Yu, W. S. Lu, C. Pan, W. B. Yao and X. D. Gao, Structure characterization, chemical and enzymatic degradation, and chain conformation of an acidic polysaccharide from *Lycium barbarum* L., *Carbohydr. Polym.*, 2016, **147**, 114–124.

28 Y. J. Gong, J. Zhang, F. Gao, J. W. Zhou, Z. N. Xiang, C. G. Zhou, L. S. Wan and J. C. Chen, Structure features and *in vitro* hypoglycemic activities of polysaccharides from different species of Maidong, *Carbohydr. Polym.*, 2017, **173**, 215–222.

29 H. X. Chen, Z. S. Wang, X. M. Lu and B. J. Xie, Isolation and chemical characterization of a polysaccharide from green tea (*Camellia sinensis* L.), *J. Sci. Food Agric.*, 2008, **88**(14), 2523–2528.

30 M. I. Pereira, A. C. Ruthes, E. R. Carbonero, R. Marcon, C. H. Baggio, C. S. Freitas, A. R. S. Santos, S. Eliasaro, G. L. Sassaki and P. A. J. Gorin, Chemical structure and selected biological properties of a glucomannan from the lichenized fungus *Heterodermia obscurata*, *Phytochemistry*, 2010, **71**(17–18), 2132–2139.

31 X. Liu, Y. Huang, Y. Chen and Y. Cao, Partial structural characterization, as well as immunomodulatory and anti-aging activities of CP2-c2-s2 polysaccharide from *Cordyceps militaris*, *RSC Adv.*, 2016, (6), 104094–104103.

32 T. Feng, Z. B. Gu and Z. Y. Jin, Structural studies of an acidic polysaccharide of Mesona blumes gum, *J. Sci. Food Agric.*, 2008, **88**(1), 24–34.

33 (*a*) X. L. Li, B. Zhang, J. Li, J. Zhou, X. L. He, L. Ye, J. Zou, C. G. Wu, X. P. Zhang and W. H. Peng, Purification, characterization, and complement fixation activity of acidic polysaccharides from *Tuber sinoaestivum*, *LWT–Food Sci. Technol.*, 2017, **85**, 82–88; (*b*) R. B. Kolsi, J. Fakhfakh, F. Krichen, I. Jribi, A. Chiarore, F. P. Patti, C. Blecker, N. Allouche, H. Belghith and K. Belghith, Structural characterization and functional properties of antihypertensive Cymodocea nodosa sulfated polysaccharide, *Carbohydr. Polym.*, 2016, **151**, 511–522.

34 L. V. Hooper, D. R. Littman and A. J. Macpherson, Interactions between the microbiota and the immune system, *Science*, 2012, **336**(6086), 1268–1273.

35 R. Pangestuti and S. K. Kim, Biological activities and health benefit effects of natural pigments derived from marine algae, *J. Funct. Foods*, 2011, **3**(4), 255–266.

36 (*a*) Z. Y. Zhu, M. Meng, H. Sun, Y. Li, Y. Y. Ren and Y. Zhang, Immunostimulatory activity of glycopeptides from *Paecilomyces sinensis* under normal and cyclophosphamide induced immunosuppressive conditions in mice models, *Food Funct.*, 2016, **7**(8), 3566–3576; (*b*) W. T. Fan, P. M. Zheng, Y. Wang, P. Hao, J. Z. Liu and X. N. Zhao,

Analysis of immunostimulatory activity of polysaccharide extracted from Yu-Ping-Feng *in vitro* and *in vivo*, *Biomed. Pharmacother.*, 2017, **93**, 146–155.

37 T. R. Mosmann and R. L. Coffman, TH1 and TH2 cells: different patterns of lymphokine secretion lead to different functional properties, *Annu. Rev. Immunol.*, 2003, **7**(7), 145.

38 X. Wang and H. Yu, Effect of *spirulina* on immunologic function of mice *in vitro* experiment, *J. Tradit. Chin. Med.*, 2004, **20**(9), 482–483.

39 W. Chen, S. Lv and D. He, The effect of *spirulina* platensis polysaccharide on lyphocyte proliferation and IFN-γ induction in immunosuppressive model mice, *Lishizhen Medicine and Materia Medica Research*, 2008, **19**(4), 941–942.

40 M. Lobner, A. Walsted, R. Larsen, K. Bendtzen and C. H. Nielsen, Enhancement of human adaptive immune responses by administration of a high-molecular-weight polysaccharide extract from the cyanobacterium *Arthrospira platensis*, *J. Med. Food*, 2008, **11**(2), 313–322.

41 Y. L. Ren, G. Q. Zheng, L. J. You, L. R. Wen, C. Li, X. Fu and L. Zhou, Structural characterization and macrophage immunomodulatory activity of a polysaccharide isolated from *Gracilaria lemaneiformis*, *J. Funct. Foods*, 2017, **33**, 286–296.

42 (*a*) P. I. Racz, M. Wildwater, M. Rooseboom, E. Kerkhof, R. Pieters, E. S. Yebra-Pimentel, R. P. Dirks, H. P. Spaink, C. Smulders and G. F. Whale, Application of *Caenorhabditis elegans* (nematode) and *Danio rerio* embryo (zebrafish) as model systems to screen for. developmental and reproductive toxicity of Piperazine compounds, *Toxicol. in Vitro*, 2017, **44**, 11–16; (*b*) T. Kaletta and M. O. Hengartner, Finding function in novel targets: C. elegans as a model organism, *Nat. Rev. Drug Discovery*, 2006, **5**, 387–399.

43 Y. S. Zhang, T. Lv, M. Li, T. Xue, H. Liu, W. M. Zhang, X. Y. Ding and Z. H. Zhuang, Anti-aging effect of polysaccharide from *Bletilla striata* on nematode *Caenorhabditis elegans*, *Pharmacogn. Mag.*, 2015, **11**(43), 449–454.

44 S. Feng, H. Cheng, Z. Xu, S. Shen, M. Yuan, J. Liu and C. Ding, Thermal stress resistance and aging effects of *Panax notoginseng* polysaccharides on *Caenorhabditis elegans*, *Int. J. Biol. Macromol.*, 2015, **81**, 188–194.

45 X. Zhao, L. Lu, Y. Qi, M. Li and L. Zhou, Emodin extends lifespan of Caenorhabditis elegans through insulin/IGF-1 signaling pathway depending on DAF-16 and SIR-2.1, *Biosci., Biotechnol., Biochem.*, 2017, **81**(10), 1908–1916.

46 Y. Chen, B. Onken, H. Chen, S. Xiao, X. Liu, M. Driscoll, Y. Cao and Q. Huang, Mechanism of longevity extension of *Caenorhabditis elegans* induced by pentagalloyl glucose isolated from eucalyptus leaves, *J. Agric. Food Chem.*, 2014, **62**(15), 3422–3431.

47 J. Lee, G. Kwon and Y. H. Lim, Elucidating the mechanism of weissella-dependent lifespan extension in *Caenorhabditis elegans*, *Sci. Rep.*, 2015, **5**, 17128.